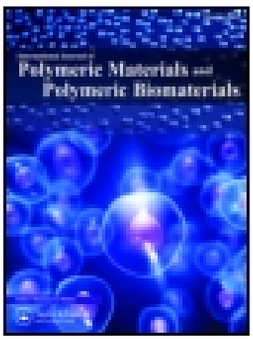

International Journal of Polymeric Materials and Polymeric Biomaterials

ISSN: (Print) (Online) Journal homepage: https://www.tandfonline.com/loi/gpom20

Selenium and clarithromycin loaded PLA-GO composite wound dressings by electrospinning method

Fatih Ciftci, Sumeyra Ayan, Nilüfer Duygulu, Yasemin Yilmazer, Zeynep Karavelioglu, Meyrem Vehapi, Rabia Cakır Koc, Mustafa Sengor, Hakan Yılmazer, Didem Ozcimen, Oguzhan Gunduz & Cem Bulent Ustundag

To cite this article: Fatih Ciftci, Sumeyra Ayan, Nilüfer Duygulu, Yasemin Yilmazer, Zeynep Karavelioglu, Meyrem Vehapi, Rabia Cakır Koc, Mustafa Sengor, Hakan Yılmazer, Didem Ozcimen, Oguzhan Gunduz & Cem Bulent Ustundag (2021): Selenium and clarithromycin loaded PLA-GO composite wound dressings by electrospinning method, International Journal of Polymeric Materials and Polymeric Biomaterials, DOI: 10.1080/00914037.2021.1925276

To link to this article: https://doi.org/10.1080/00914037.2021.1925276

Published online: 18 May 2021.

INTERNATIONAL JOURNAL OF POLYMERIC MATERIALS AND POLYMERIC BIOMATERIALS
https://doi.org/10.1080/00914037.2021.1925276

Selenium and clarithromycin loaded PLA-GO composite wound dressings by electrospinning method

Fatih Ciftci[a,b], Sumeyra Ayan[a,c], Nilüfer Duygulu[d], Yasemin Yilmazer[e], Zeynep Karavelioglu[a], Meyrem Vehapi[a], Rabia Cakır Koc[a], Mustafa Sengor[f,g], Hakan Yılmazer[d], Didem Ozcimen[a], Oguzhan Gunduz[f,g], and Cem Bulent Ustundag[a]

[a]Department of Bioengineering, Yildiz Technical University, Istanbul, Turkey; [b]Technology Transfer Office (TTO), Fatih Sultan Mehmet Vakif University, Istanbul, Turkey; [c]Materials Institute, Marmara Research Center, TUBITAK, Gebze, Turkey; [d]Department of Metallurgical and Material Engineering, Yildiz Technical University, Istanbul, Turkey; [e]Department of Molecular Biology and Genetics, Istanbul Sabahattin Zaim University, Istanbul, Turkey; [f]Center for Nanotechnology and Biomaterials Application and Research (NBUAM), Marmara University, Istanbul, Turkey; [g]Department of Metallurgical and Materials Engineering, Marmara University, Istanbul, Turkey

ABSTRACT

Diabetic wounds are very problematic wounds that have a high risk of infection. The healing process of wounds in diabetic patients is more complicated than others. Wound dressing preparation is one of the promising treatment modalities for repairing damaged tissues in diabetic patients. The aim of this study is to demonstrate the antibacterial effects of drug release of clarithromycin from poly(lactic acid) (PLA) nanofibers incorporated with selenium (Se) and graphene-oxide (GO) to reveal their wound healing potential. In the present study, optimized PLA was combined with graphene oxide (GO) with a concentration of 0.45 wt%, 1 wt%, 1.50 wt%, 2 wt%, 2.50 wt%, and 3 wt%, respectively, and the combination was produced by modified Hummers method. After that, optimized PLA/GO was incorporated with Se and clarithromycin with PLA with the percentage by weight of 1:1, nanofiber patches were successfully produced by the electrospinning technique. *In vitro* antibiotic test, cell culture tests (cytotoxicity test, cell adhesion, and *in vitro* wound healing assay), morphological analysis (SEM), molecular interactions between the components (FT-IR), tensile strength, and physical analysis (viscosity, surface tensile, density and conductivity tests) were carried out after production of nanofiber patches. According to the results, the average pore size of 8 wt% PLA + 1 wt% GO + 1 wt% Se + 1 wt% clarithromycin nanofiber is 640 nm. Moreover, 8 wt% PLA + 1 wt% GO + 1 wt% Se + 1 wt% clarithromycin has the highest viscosity and surface tension value than others with the values of 253.8 ± 6.67 mPas and 31.62 ± 2.13 mN/m, respectively. Finally, it was observed that Se-incorporated electrospun nanofibers had antibacterial effects and are highly promising wound healing materials. To sum up, the prepared nanofibers illustrated important suitable mechanical properties, controlled release and antibacterial effect and results showed that Se incorporated PLA-GO-drug composite is a promising wound healing material.

GRAPHICAL ABSTRACT

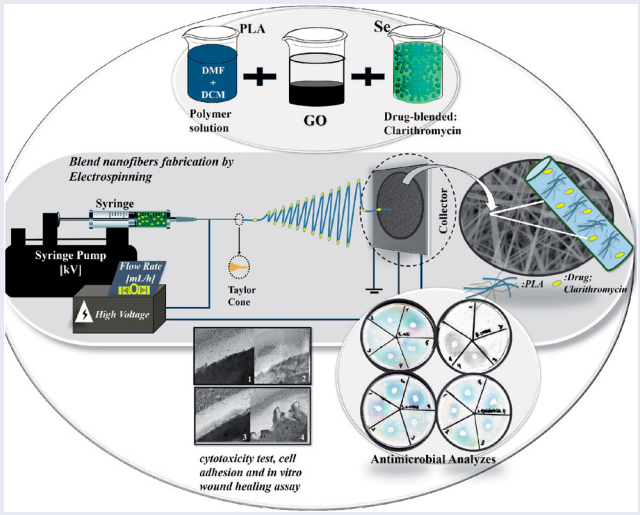

ARTICLE HISTORY

Received 21 December 2020
Accepted 29 April 2021

KEYWORDS

Drug; electrospinning; graphene oxide; selenium; wound dressing

CONTACT Cem Bulent Ustundag cbustun@yildiz.edu.tr, cbustundag@gmail.com Department of Bioengineering, Yildiz Technical University, Istanbul, Turkey.

1. Introduction

Diabetic foot ulcer is a chronic and non-healing wound that is able to lose limb[1]. Chronic wounds do not follow well-defined healing sequence as a normal healing process, it is more complicated due to different biochemically, and different growth factors, matrix metalloproteases, and diverse proteins. Hypothermia is effective to obtain vasoconstriction, however, it causes some problems such as going down cutaneous blood flow, insufficient oxygenation, and impaired immune function. Moreover, reduced sweat production causes peripheral autonomic neuropathy gives the skin dry and fragile so that bacteria are able to enter into the skin easily[2].

Electrospinning method is one of the effective methods for producing a wound dressing material due to its several advantages. The process of spinning nanofibers or nanoparticles with the use of electrostatic forces is known as electrospinning technique[3]. Solution parameters (viscosity, conductivity, and surface tension), process parameters (applied electric field, tip to collector distance, and feeding or flow rate), and ambient parameters (humidity and temperature of the surrounding) play an important role in desired morphology and diameters of nanofibers. Electrospun nanofibers offer many advantages compared to conventional wound dressing materials. These advantages can be listed as controlling the fiber size during production, absorbing wound exudate, and allowing wound healing due to their large surface areas and encapsulation efficiencies[4–7].

Poly (lactic acid) (PLA), which is a thermoplastic polymer, is a preferred biopolymer due to its renewability, biodegradability, and relatively low cost[8]. PLA is widely used for different purposes such as surgical implant materials[9], scaffolds for tissue engineering[10], drug delivery systems[11], chemical and optical sensors[6], wound dressing materials[12], and dental applications[10]. PLA-based antimicrobial materials attract great attention as promising systems for controlling microbial growth. In addition, PLA is a very suitable polymer that can be utilized as a wound dressing material due to its low immunogenicity and good mechanical properties[13].

Graphene is a free-standing two-dimensional crystal with one-atom thickness[14]. Recent studies have shown that understanding graphene-cell (or tissue, organ) interactions; particularly the cellular uptake mechanisms are still challenging[9]. It can be theoretically viewed as a true planar aromatic macromolecule[14], and it is degraded by peroxidases[15]. Biosafety of graphene and graphene derivatives is attracting more and more attention as we need to learn the fate of graphene and its derivatives *in vivo* once it invasively enters into a biological system. It has now been accepted that the biological effect of graphene is complex and largely affected by the exposure dose and methods as well as the chemical functionalization, lateral size, thickness, and surface properties[9]. Due to its high mechanical resistance, chemical stability, large surface area, low toxicity[20], high drug loading capacity, and antibacterial properties[15], graphene oxide (GO) has had widely used in biomedical applications[16].

In this study, Selenium (Se) was used which has novel antibiotic chemistry that lacks known bacterial resistance[17–19]. Se is mostly found in selenoproteins (as selenomethionine), which has an important anti-oxidants[20] and anti-inflammatory effect. Selenium is a common trace element in the body and has been an important active ingredient in the formation of selenoproteins in particular[21,22]. Se has been suggested to have anticancer effects[23]. Various examinations have been performed to understand the relationship between Se levels and conditions like oxidative stress and inflammation because of diabetes mellitus, results showed that Se has a positive effect on diabetes mellitus due to antioxidative and anti-inflammatory characteristics of Se[24]. The concentration of selenoprotein P in plasma is known to be higher in patients with type 2 diabetes (T2D). Nevertheless, serum albumin that transports selenomethionine is decreased in diabetes. Expression of selenoprotein P is known to be decreased during the inflammation phase. Therefore, Se levels in the blood are reduced by systemic response during the inflammation phase that is occurred in T2D. Se supplementation may cause insulin resistance has not been determined yet, even if some hypotheses are available. Se is believed to be beneficial in relation to glucose homeostasis, and decrease insulin resistance[25].

Clarithromycin has a broad spectrum of antimicrobial activity and inhibits a number of Gram-positive and Gram-negative organisms, atypical pathogens and some anaerobes[26]. Clarithromycin has a superior pharmacokinetic profile[27,28]. Clarithromycin improved pharmacokinetic profile and in vitro antimicrobial activity reveal superior efficacy in infectious diseases[29,30]. It is susceptible to strains of *S.aureus and S. epidermidis*[31]. Clarithromycin is the most potent macrolide tested against *Bacillus* species and is more active against *Listeria monocytogenes*[32].

The aim of this study is to determine the wound healing effect of Se-incorporated PLA-GO nanofibers. Antibacterial activity and *in vitro* wound healing effects of the nanofibers from blends of PLA and GO were examined. According to the results, the prepared nanofibers had good mechanical properties and antibacterial test and *in vitro* wound-healing assay showed that Se incorporated PLA-GO-drug composite is a promising wound healing material.

2. Materials and methods

In the present study, PLA − 4060 D (MW ∼ 92 kDa), polymer was used in granule form. The solvents used in this study were; N, N dimethylformamide (DMF, Mw = 73.09 g/mol, Merck) and dichloromethane (DCM, Mw = 84.93 g/mol, Merck). These solvents were selected due to their similar solubility parameters to PLA. All the solvents were purchased from Merck and used without further purification. Graphene oxide synthesis was carried out by the modified Hummers method. Se (Mw = 78.96, Sodium selenite CAS-10102-18-8 Santa Cruz) was purchased from Merck in powder form and Clarithromycin (C38H69NO13, MW: 747.95 CAS no: 81103-11-9 Abbott Laboratories, Illinois, United States) was purchased from Merck. All nanofibers

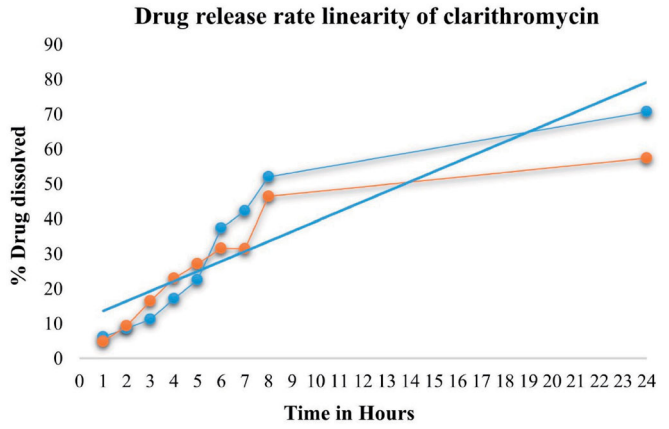

Figure 1. Drug release rate and linearity of clarithromycin from PLA-NF patches.

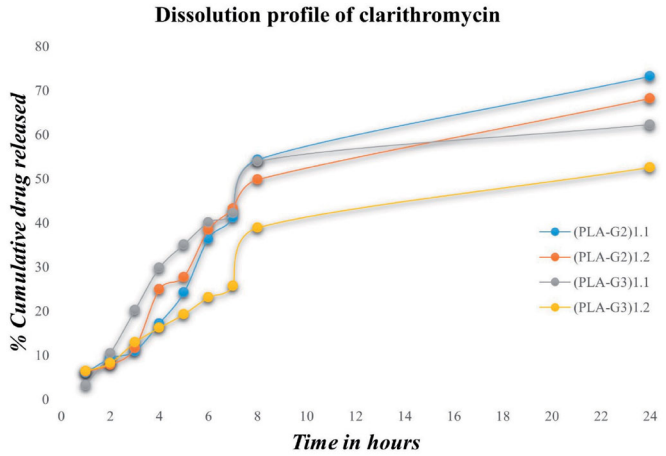

Figure 3. Cumulative drug release rates profile of clarithromycin from PLA-NF patches.

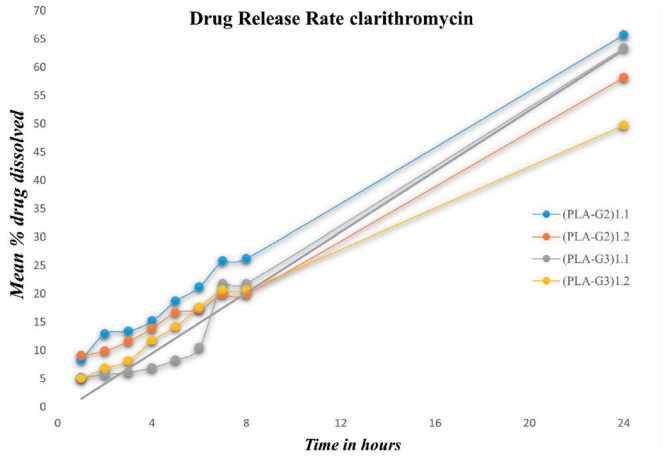

Figure 2. Drug dissolution rates PLA-NF profile in PBS.

production processes in this study were carried out by electrospinning (Fytronix ESP 9000, Turkey) method.

According to the correlation coefficient, both linearity (linear), drug release kinetics, and similarities and differences with an approach independent of the drug model were compared by determining the mathematical model of drug release kinetics and dissolution profiles. By taking two samples for PLA-G2 and PLA-G3 used for release, the mean value, cumulative and dissolution times, and values in PBS were finally obtained (Figures 1–3).

Statistical analyzes were made and compared to antibacterial studies (Figure 4). (a) Antibacterial effects of nanocomposite films containing PLA-G3 at 24 h against *E.coli*. (b) Inhibition zones produced by different nanocomposite films against *E.coli*. (c) Antibacterial effects of nanocomposite films containing PLA-G3 at 24 h against *S. aureus*. (d) Inhibition zones produced by different nanocomposite films against *S. aureus*. (e) Antibacterial effects of nanocomposite films containing PLA-G3 at 24 h against *B. cereus*. (f) Inhibition zones produced by different nanocomposite films against *B. cereus*. (g) Antibacterial effects of nanocomposite films containing PLA-G3 at 24 h against *S. epidermidis*. (h) Inhibition zones produced by different nanocomposite films against *S. epidermidis*. All experiments were carried out in triplicates. Analyses included the use of ANOVA independent-samples t-test. Differences were determined to be significant at $p < 0.05$. Results were expressed as mean ± standard deviation. The statistically significant difference between the mean will be calculated by one-way ANOVA with the level of significance to be selected at $p < 0.05$.

2.1. Preparation of electrospun poly-lactic acid nanofibers (PLA-NF)

The electrospinning process was carried out at 3, 5, and 8% wt/v PLA polymer concentrations by using double solvent systems at different ratios. Firstly, PLA particles were dissolved in DMF, and then DCM was added to the solution and stirred for 2 hours. The amount of both PLA and DMF was kept constant, and the polymer concentrations were determined among the solvent ratio variations. The solvent ratios of DMF, DCM were changed as: 1:3 v/v for 3% wt/v, 1:1 v/v for 5% wt/v and 0.5:0.5 v/v for 8% wt/v PLA polymer concentrations, respectively.

Synthesized GO is added with different weight percentages (0.45, 1, 1.5, 2, 2.5, and 3 wt%) into the solution. Then only for 8 wt/v PLA, Se and clarithromycin were added into the solution with respect to 1% wt of PLA. Based on the typical electrospinning process, the suspension was drawn into the 10 mL plastic syringe with a stainless steel needle. Prepared 8 wt%; PLA, PLA + 1 wt% GO (PLA-G), PLA + 1 wt% GO + 1 wt% Se (PLA-G1), PLA + 1 wt% GO + 1 wt% clarithromycin (PLA-G2) and PLA + 1 wt% GO + 1 wt% Se + 1 wt% clarithromycin (PLA-G3) solutions were utilized for electrospinning to produce nanofibers. Parameters of the electrospinning process were set as the voltage was 25 kV, a rotational speed of the collector electrode was 999 rpm, the distance was 15 cm and the feeding rate was 4000 µL/h. At 37 °C around 50% humidity and other electrospinning process parameters were common for all cases.

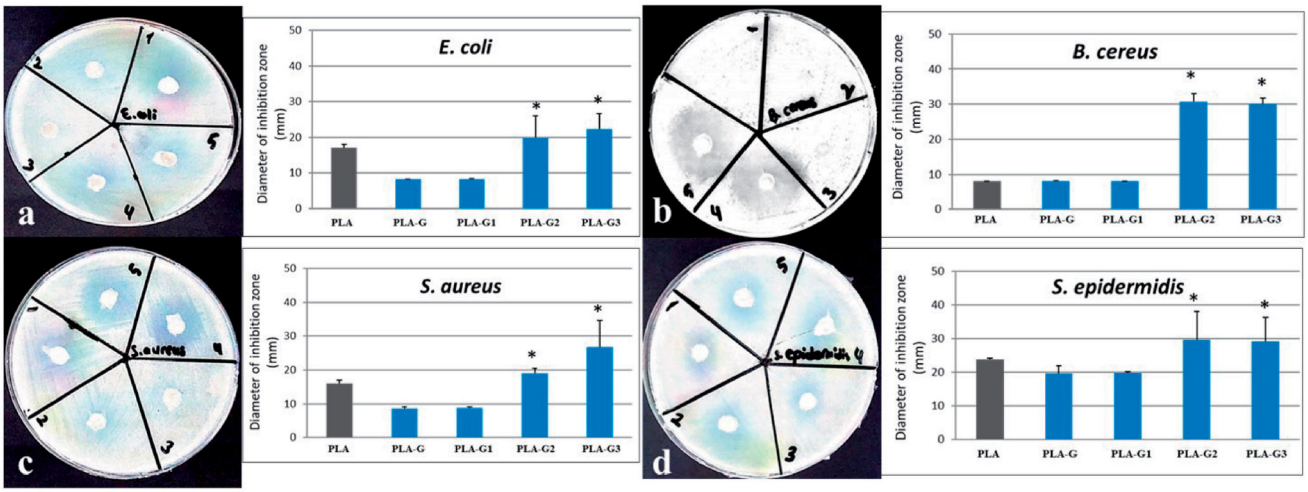

Figure 4. Disk diffusion analysis of nanocomposite films containing PLA-G3 for (a) *E. coli*, (b) *B. cereus*, (c) *S. aurus*, and (d) *S. epidermis*.

3. Characterization

3.1. Physical characterization

The characterization of fibers that were produced by the electrospinning technique is the most significant part of electrospinning process in order to determine the properties of the fiber. Density, electrical conductivity, surface tension, and viscosity values were measured to determine the physical characterization of the prepared electrospinning solutions. Density was measured by using a standard 10 mL bottle. The electrical conductivity was measured using the Cond 3110 SET 1, WTW, Germany. The surface tension was measured using a force tensiometer Sigma 703 D, Attention, Germany. The viscosity was determined using a DV-E, Brookfield AMETEK, USA instrument. All the experiments were carried out at room temperature (23 °C).

3.2. Morphology and structure

The morphological analysis of all produced nanofibers was carried out by scanning electron microscopy (SEM) (EVO LS 10, ZEISS). The working conditions were 15 kV and mode of secondary backscattered electrons. All the samples were coated with gold-palladium to ensure conductivity since the polymers lack of this property.

All samples were chemically characterized by Fourier-transform infrared (FTIR) spectroscopy on an IR Affinity-1 infrared spectrophotometer (Jasco, FT/IR-4700 type A) in a range of 449.333–4,000.6 cm^{-1} and averaged over 32 scans with 4 cm^{-1} resolution in transmittance mode using the KBr pellet method. Detector of FTIR is TGS.

Before the tensile strength tests, each sample was placed onto rectangular-shaped surfaces which are 5 cm in length and 1 cm in width. The thickness of each test specimen was measured using a high-accuracy digital micrometer (Mitutoyo, USA). The tensile strength and strain of electrospun nanofibers were performed using a tensile tester (Shimadzu, Japan) by means of running special software. All samples were subjected to test the speed of 5 mm/min until the breaking point. The measurements were carried out at room temperature (23 °C).

4. *In vitro* release study

Various formulations, respectively samples; PLA-G2 and PLA-G3 were selected for drug release studies. Drug release of clarithromycin from PLA-NF was estimated by the dialysis cell membrane method in two different media, respectively phosphate buffer saline (PBS) (pH 7.4) at 37 ± 1 °C for 24 h under sink condition. Appropriate volume of nanofibers dialysis was taken in the dialysis tube against 100 mL of media, continuously stirred with a magnetic stirrer at 37 ± 1 °C.

Appropriate volume of PLA-NF dialysis was taken in dialysis tube against 100 mL of media, continuously stirred with magnetic stirrer at 37 ± 1 °C. After appropriate time intervals (1 h) one mL sample was withdrawn and analyzed for drug content at 770 nm, in a UV/Vis Spectrometer (Lambda 35; PerkinElmer, Germany). An equal volume of fresh media preheated to 37°Cwas added to replace the withdrawn sample. The stability of PLA-NF was evaluated in with PBS (pH 7.4) and in SGF (pH 1.2). Ten milligrams of formulations were incubated at 37 ± 1 °C with 20 mL of PBS (pH 7.4) and SGF (pH 1.2), for a period of 2, 4, 8, and 24 h. After specified time intervals, the suspension was centrifuged at 15,000 rpm for 1 h, the supernatant was removed and nanoparticles were dissolved in ethanolic solution (7:3 ratio). PLA-NF content was determined by taking absorbance at 220.3 nm against blank. Cumulative % release of clarithromycin all the formulations was determined by storage in amber-colored vials, closed with rubber closers at room temperature, 0 °C and at 4 °C and % residual clarithromycin contents were determined after 10, 20, and 30 d.

4.1. Cell culture

L929 cells were obtained from ATCC. Dulbecco's Modified Eagle's Medium 12 (DMEM/F12), Fetal Bovine Serum (FBS), Trypsin-EDTA (0.25%), and Trypan Blue were

obtained from Gibco. Penicillin-streptomycin antibiotic solution (GeneMark), Phosphate Buffer Saline (PBS) tablets, XTT (2,3-bis-(2-methoxy-4-nitro-5-sulfophenyl)-2H-tetrazolium-5-carboxanilide, and Phenazine Methosulfate (PMS) were obtained from Santa Cruz Biotechnology.

L929 cells were used for *in vitro* cell culture experiments. Ethical approval is not necessary for the standard cell lines. The cell lines were cultured in DMEM/F12 medium (supplemented with 10% fetal bovine serum and penicillium–streptomycin 0.5% from 10,000 units mL^{-1} Penicillin–10 mg mL^{-1} Streptomycin) and incubated at 37 °C in 5% CO_2. The confluent culture was trypsinized to detach cells from the surface and centrifuged at 1,000 rpm for 5 min. The supernatant was discarded, and the cell number in the pellet was counted with a hemocytometer. Subsequently, cells were prepared for cytotoxicity, cell adhesion, and scratch assay experiments.

5. Cytotoxicity experiments

5.1. Direct Contact method

Samples were placed into the wells then L929 cells with a concentration of 3×10^4 in 500 µL of medium were seeded in each well of 48-well flat-bottom microplates and incubated at 37 °C for 24 h for cell attachment. After 24 h of the incubation period, all volume of the culture media was aspirated then the medium was replaced with 500 µL fresh medium containing 2,3-bis-(2-methoxy-4-nitro-5-sulfophenyl)-2H-tetrazolium-5-carboxanilide (XTT) with a concentration of 0,5 mg/mL (with 7.5 mg/mL phenazine methosulfate). The cells were incubated for 4 h at 37 °C, the cell culture medium was used as a negative control. Optical density was measured at 450 nm and the percentage of cell viability was calculated.

5.2. Indirect method

Samples were kept in the cell culture medium for 24 h and the effect of different volumes of the medium (25 µL, 50 µL, 75 µL, 100 µL) on the cell viability was tested on L929 cells seeded in 96-well plates. After 24 h of incubation period, standard XTT assay was performed and percentage of cell viability was calculated according to the following Formula (1)[24]:

$$\%Cellviability = \frac{Opticaldensityofsample}{Opticaldensityofcontrol} \times 100 \qquad (1)$$

5.2.1. Cell adhesion

Samples were placed into the wells then L929 cells with a concentration of 5×10^4 in 1 mL of medium were seeded in each well of 24-well flat-bottom microplates and incubated at 37 °C for 24 h for cell attachment. After 24 h of the incubation period, cell adhesion on the samples was observed via microscope.

5.2.2. In vitro wound healing assay (scratch assay)

L929 cells with a concentration of 3×10^4 in 500 µL of medium were seeded in 48-well flat-bottom microplate and incubated at 37 °C for 24 h. After the cells were confluent on the surface of the plate bottom, "plus-shaped" scratches were created on wells then samples were added to each well. Then the pictures from the cells were taken at certain intervals (3 h, 6 h, 12 h, and 24 h) until the scratches were closed. The effect of the samples on cell migration was evaluated visually according to the wound closure time.

5.2.3. Antimicrobial analyzes

The disk diffusion test was performed to determine the antibacterial activity of the nanocomposite films[33]. *E. coli* (ATCC 25922), *S. aureus* (ATCC 25923), *B. cereus* (ATCC 11778), and *S. epidermidis* (ATCC 12228) suspensions were collected from 18 h nutrient broth cultures then adjusted to 0.5 McFarland standard turbidity (1.5×10^8 CFU/mL) and diluted (1:10) to the desired bacterial density. Mueller-Hinton agar plates inoculated with 0.1 mL of the bacterial suspensions (1.5×10^6 CFU/mL). The nanocomposite films were sliced into 7 mm segments and sterilized with UV for 2 h and subsequently placed on bacteria plated petri dishes. The plates were incubated at 37 °C for 24 h, after which the inhibition zones around the disks were measured by a digital micrometer[34]. To choose the optimum nanocomposite film, four separate groups were prepared and tests were performed three times. The antibacterial study content is given in Figure 4. The numbers on the disks are 1, 2, 3, 4, 5 respectively; The sample was designated as PLA, PLA + GO (PLA-G), PLA + GO + Se (PLA-G1), PLA + GO + clarithromycin (PLA-G2) and PLA + GO + Se + clarithromycin (PLA-G3). Inhibition growth values (mm) are given as histogram by taking 3 different measurements for each number.

6. Result and discussion

Increasing concentration, thereby solution viscosity, was resulted in larger and more uniform fiber diameters. Morphology of the beads formed on the fibers altered from spherical to spindle-like and ultimately uniform fibers with increased diameters are formed due to the higher viscosity resistance. The solution with the high surface tension blocks the electrospinning process due to the instability of the jets and the generation of sprayed droplets. Fiber diameter and concentration are directly proportional to each other. When concentration is increased, fiber diameter is also increased. When the electrospinning process is performed another very important parameter is the applied voltage to the solution. Only after the access of threshold voltage, fiber formation occurs, this contains the necessary charge on the solution along with the electric field and starts the electrospinning technique. Taylor[35] determined that the critical value of voltage must be 6 kV. When the voltage value was smaller than this critical value, the fiber formation became difficult. While, at very high voltage applications, the stability of the

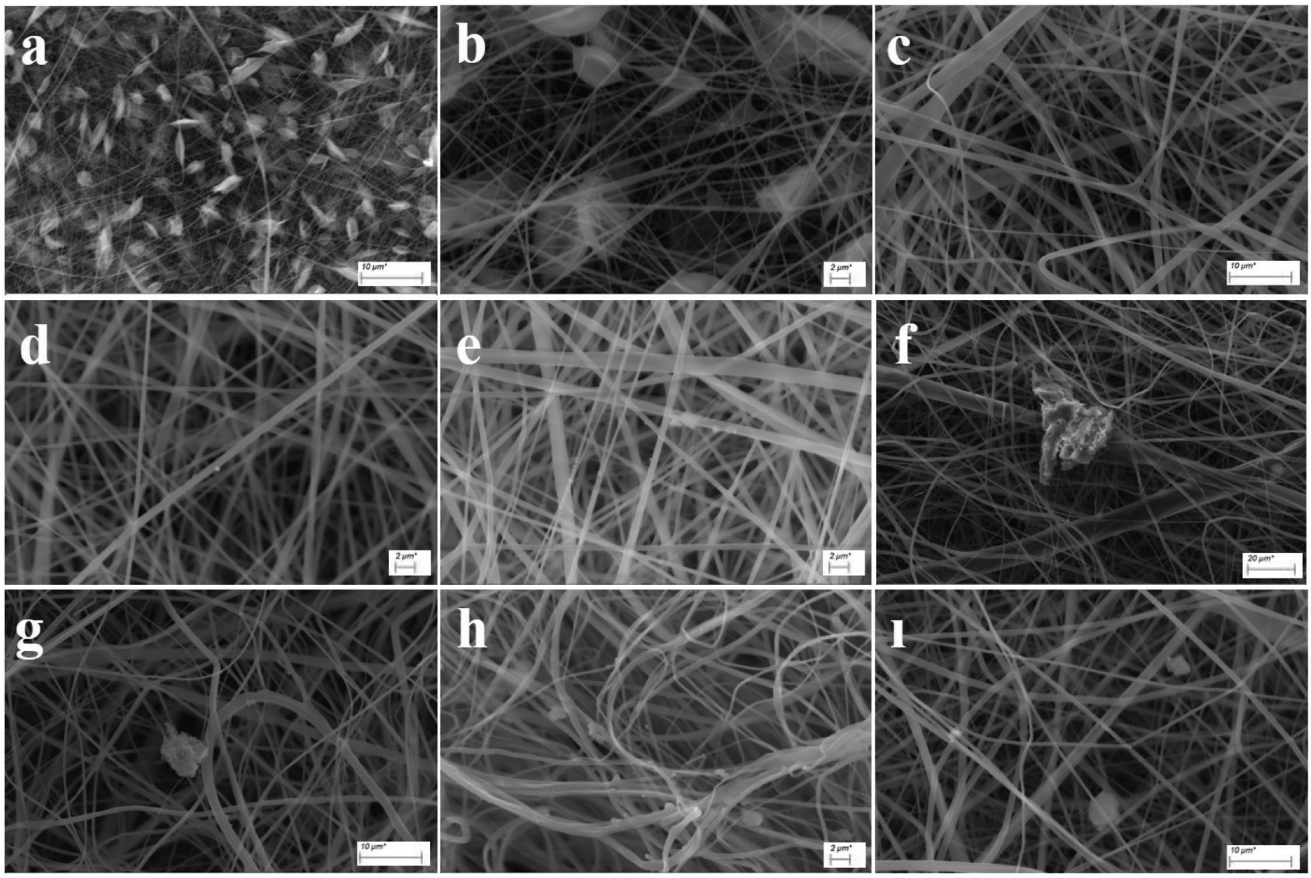

Figure 5. SEM images of PLA with different concentrations (a) 3 wt% PLA, (b) 5 wt% PLA, (c) 8 wt% PLA and SEM images of different GO concentrations with 8% PLA (d) 8 wt% PLA + 0.45 wt% GO, (e) 8 wt% PLA + 1 wt% GO, (f) 8 wt% PLA + 1.50 wt% GO, (g) 8 wt% PLA + 2 wt% GO, (h) 8 wt% PLA + 2.5 wt% GO, and (ı) 8 wt% PLA + 3 wt% GO.

Table 1. The result of physical characterization of solutions and fibers as samples.

Sample (S)	Viscosity (mPas)	Surface tensile (mN/m)	Density (g/mL)	Conductivity (μS/cm)	Average fibers diameter (nm)
PLA	123.0 ± 6.90	30.28 ± 2.21	1.2184	2.6	541.56 ± 94.19
PLA-G	104.6 ± 8.50	28.95 ± 2.18	1.2205	15.3	472.66 ± 183.38
PLA-G1	247.9 ± 8.60	30.72 ± 1.25	1.2349	8.5	354 ± 154.12
PLA-G2	251.4 ± 6.81	27.94 ± 1.21	1.2256	9.7	414.03 ± 201.85
PLA-G3	253.8 ± 6.67	31.62 ± 2.13	1.1761	14.7	642 ± 173.79

Measuring repetition amounts; (valid for each sample); for viscosity; 5, for surface tensile; 3, for density; 3, for conductivity; 4, for average diameter; 200.

polymer jet advancing to the collector surface may disrupt and it may induce bead formation due to the increment of solution surface tension or charge density[36–39]. Another important parameter of electrospinning is the flow rate of the polymer jet. A fast flow rate may prevent the nanofiber jet completely drying, and this leads to an increase in the fiber diameter. On the other hand, a very slow flow rate may induce beads formation. Additionally, ribbon-like defects and unspun droplets may occur at high or low flow rates. Therefore, the flow rate of the electrospinning process must be optimized to achieve uniform and beadless electrospun nanofibers[40–43]. Studies have been depicted that when higher voltages are applied to the solution, there is more polymer ejection. Therefore, we can say that nanofibers occur with a larger diameter. Moreover, most cases illustrate that a higher voltage leads to greater stretching of the solution because of the greater coulombic forces in the jet as well as a stronger electric field. We applied 25 kV voltage to the prepared solution. According to Figure 5, it can be depicted that GO had a smoothing effect on the PLA fibers which resulted in bead-free morphologies. Since beads are the stress-raising places for cells, GO addition is a suitable backbone for the incorporation of other functional agents. The result of the physical characterization of solutions is illustrated in Table 1. Repeat amounts for all measurements are listed under Table 1. It shows that the average diameter for PLA is 541.56 ± 94.19 nm and the average diameter of PLA-G is 472.66 ± 183.38 nm. The added substance variability in the solution changed both the viscosity and the surface tension. The increase in viscosity caused the formation of bead structure in fiber morphology. Consequently, the morphology of beads alters from spherical to spindle-like and ultimately uniform fibers with increased diameters are formed due to the higher viscosity resistance. The solution

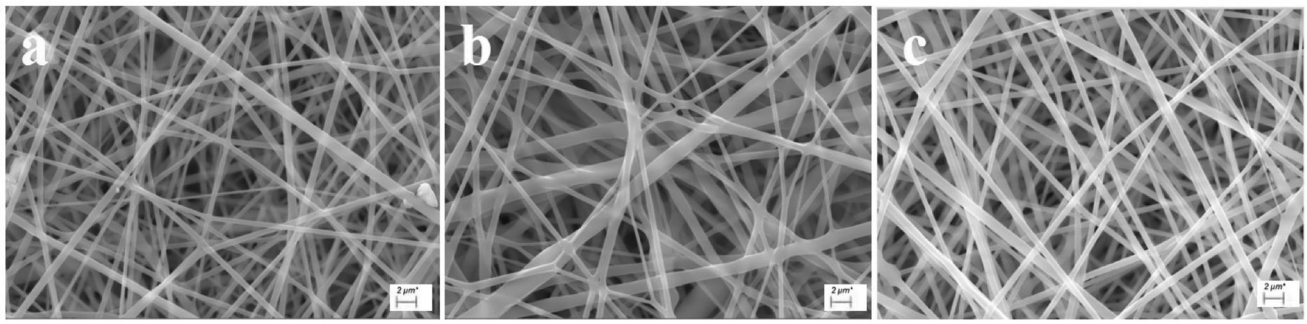

Figure 6. SEM images with 2 μm size of (a) PLA-G1, (b) PLA-G2, and (c) PLA-G3.

with the high surface tension blocks the electrospinning process due to the instability of the jets and the generation of sprayed droplets. Fiber diameter and concentration are directly proportional to each other as in the literature[6]. When concentration is increased, fiber diameter is also increased.

According to SEM images which are illustrated as in Figure 5, PLA-G solution was chosen, which is well-distributed due to enough stirring, in order to load either Se or clarithromycin. Stirring is important for obtaining nanofiber when we used GO in dash form. SEM images of PLA-G1, PLA-G2, and PLA-G3 are illustrated as in Figure 6. The diameter of nanofiber and the solution concentration used in electrospinning are directly proportional to each other. The average diameter of nanofiber patches is as shown in Table 1. With the addition of GO and Se, fiber diameter was reduced in nanofiber patches. The lowest fiber diameter (354 ± 154.12 nm) was observed in PLA-G1. When concentration is increased, fiber diameter is also increased. The morphology of beads alters from spherical to spindle-like and ultimately uniform fibers with increased diameters are formed due to the higher viscosity resistance. The average diameters of PLA-G3 nanofibers were 642 ± 173.79 nm. Moreover, PLA-G3 has the highest viscosity and surface tension value than others 253.8 ± 6.67 mPas and 31.62 ± 2.13 mN/m, respectively. Besides, the presence of polar groups on the surface of this material improves the compatibility. On the other hand, cytotoxicity and cell adhesion experiments showed the materials' low toxicity potential, biocompatibility. The inhibition rates of the PLA-G2, and PLA-G3 on *E. coli*, *S. aureus*, and *B. cereus* had higher than other formulation groups. It is shown that PLA-GO nanofibers combined with clarithromycin have a stronger antibacterial effect. Cell culture experiments showed that all five samples support the cell adhesion, and according to the *in vitro* wound healing experiment, cells exposed to samples had a faster cell migration compared to the control group. As a result, a faster wound healing situation was observed by supporting PLA-GO nanofibers with Se. Besides, supporting nanofibers with clarithromycin resulted in the production of an antibacterial effect in the wound environment.

Here, we have added Se nanoparticles to give PLA antibacterial properties, to electro spin PLA loaded with clarithromycin and GO. We have described a morphology similar to ECM with PLA/GO/Se/clarithromycin nanofibers. Se-doped PLA showed antibacterial[44], antimicrobial[45], antioxidant[46] effects with nanofiber groups. Chung et al.[44] It has also been shown in the Se supplemented PCL study that it inhibits bacteria and reduces bacterial cell activity in skin applications. The addition of Se as a contribution to PLA nanofibers has shown in this study that it has the potential of wound dressing as a biomedical application that increases wound healing and reduces infection in the absence of antibiotics.

The stress-strain % curves (Figure 7) values of nanofibers at break were examined at room temperature (23 °C). Such results are important for determining the flexibility of the final product. When the fibers were compared with the tensile test, it was observed that the fibers could not adhere to each other and therefore their mechanical properties were reduced[47]. It was observed that the ductility of the material decreased and the mechanical strength increased with the addition of GO. Zhang et al.[48] In their study, it was observed that the addition of GO greatly improved tensile stress, but ductility decreased with low elongation at break. Davoodi et al.[49] In their study, it was observed that a strong matrix interaction of GO nanosheets with PLA caused an increase in the strength of PLA-GO fibers.

PLA-G was seen as the best of other NFs mechanically with its 7.2 ± 0.25 MPa value. PLA-G1 has a very low load-carrying capacity with a value of 2.2 ± 0.50 MPa and does not flex under load. It has been observed that PLA-G2 has a better load carrying capacity with a value of 5.6 ± 1.75 MPa, but it may show a risk of fracture in biomedical use areas since it does not show enough elongation under load. PLA-G3, with a value of 3.8 ± 0.50 MPa, has been analyzed to be able to respond better to loads from different directions in terms of formability, as its load-bearing is less, but its elongation is better. As a result, PLA-G1, PLA-G2, and PLA-G3 can be used if they are to be used for areas that will contact the body surface, i.e., epithelial tissue, according to biomedical application areas. The selection criteria of the NLs vary according to the place of application. For applications with low load and unidirectional force, even the PLA-G1 may be sufficient. PLA-G has been deemed sufficient for higher-level applications.

FTIR analysis was carried out to investigate the functional groups of electrospun nanofiber patches as granulated clarithromycin, granulated GO, granulated selenium, electrospun nanofiber patches shows as Figure 8. PLA had a transmission band at 2150 cm^{-1}. C–O stretching, C=O stretching, C-H bending, and -CH stretching band structures

are shown in Figure 8. PLA-NF the nanofiber patches had an absorption band at around 2150 cm^{-1} and bands between 1980 and 700 cm^{-1}.

6.1. Cytotoxicity Experiments

6.1.1. Direct and indirect contact method

When the effect of the samples on L929 cell viability via direct contact method is examined; It was observed that PLA-G1, PLA-G2, PLA-G3 showed a weak cytotoxic effect while

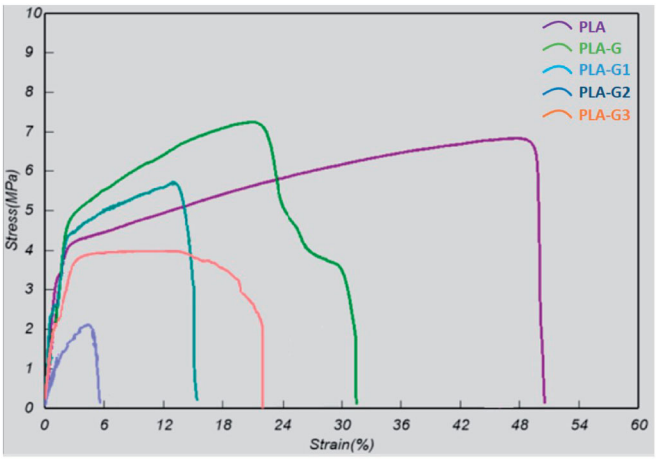

Figure 7. Stress–strain curves of PLA, PLA-G, PLA-G1, PLA-G2, PLA-G3 nano fibers.

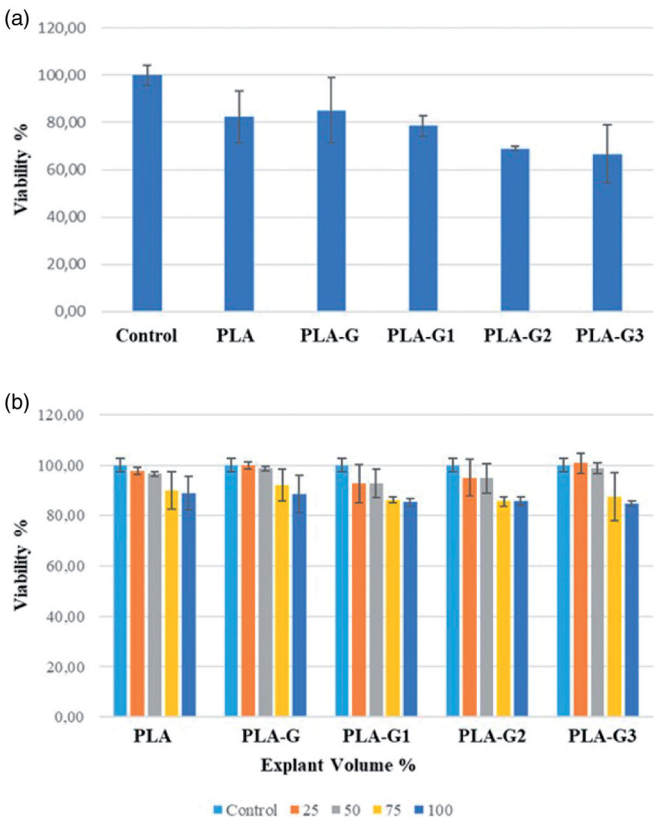

Figure 9. (a) Effect of the samples on L929 cell viability via direct contact method, (b) effect of samples; PLA, PLA-G, PLA-G1, PLA-G2, PLA-G3.

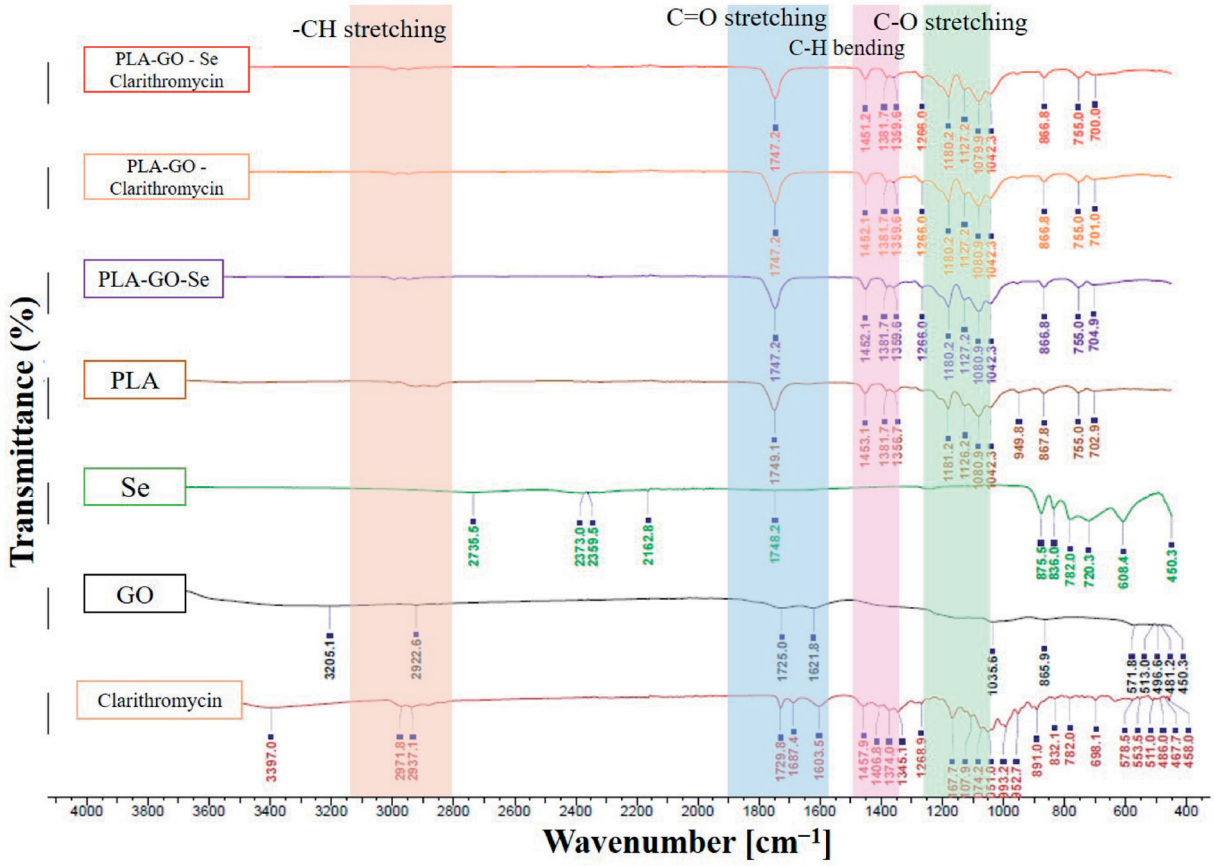

Figure 8. FTIR spectrum of granulated clarithromycin, granulated GO, granulated selenium, nanofiber form of samples.

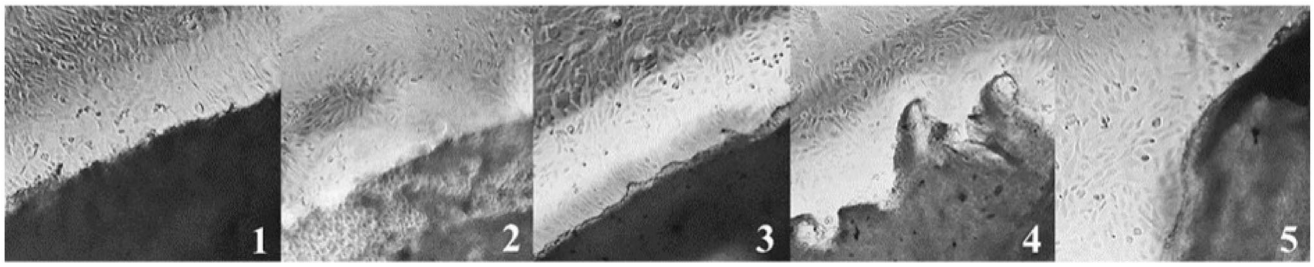

Figure 10. Cell adhesion on samples; 1. PLA, 2. PLA-G, 3. PLA-G1, 4. PLA-G2, 5. PLA-G3.

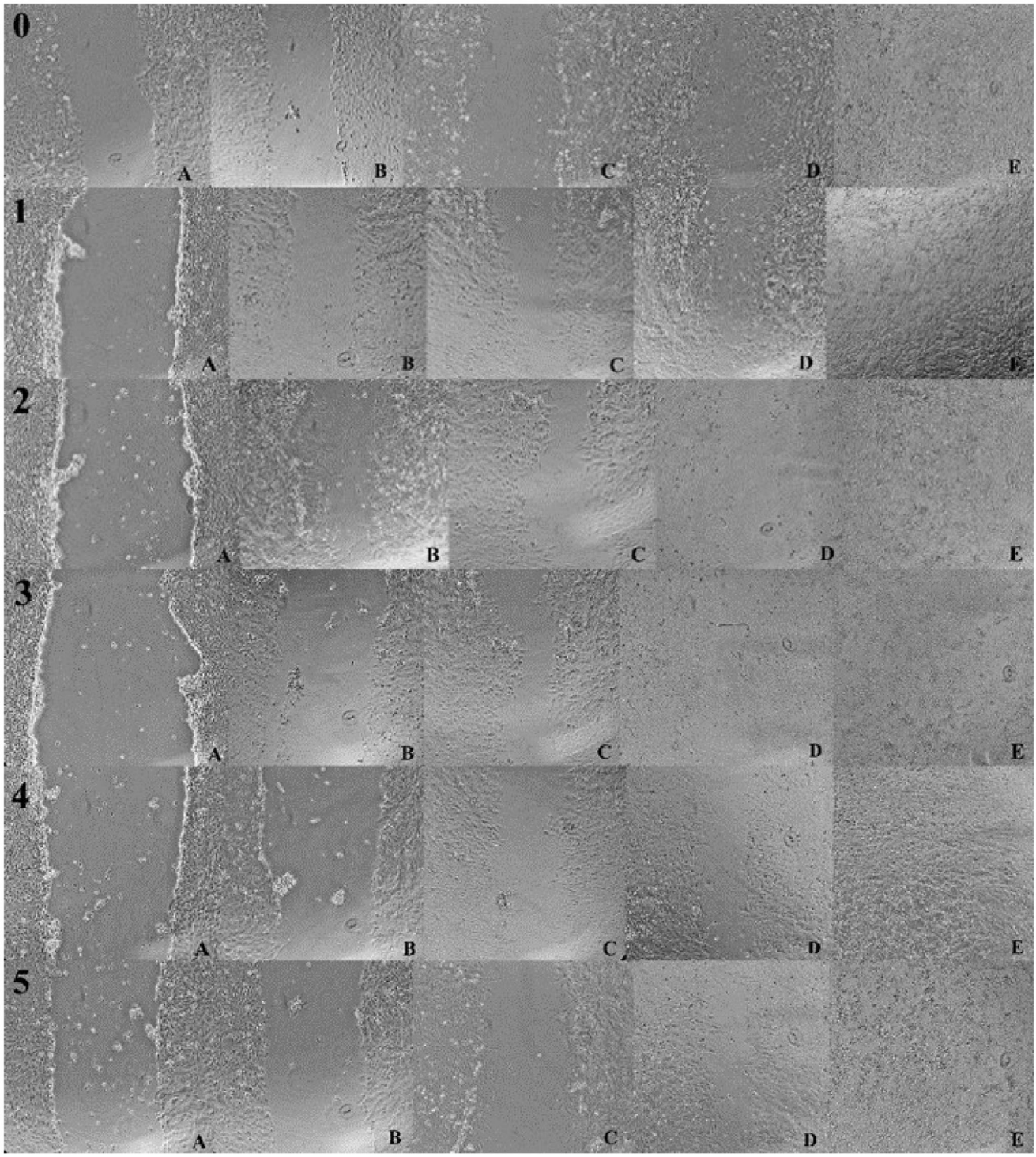

Figure 11. Control Group (0) and Effects of samples; 1. PLA, 2. PLA-G, 3. PLA-G1, 4. PLA-G2, 5. PLA-G3 on L929 cell migration. A: 0 h, B: 3 h, C: 6 h, D: 12 h, E: 24 h.

PLA and PLA-G did not show a toxic effect on the cells (Figure 9) according to the ISO 10993-5 standards[27]. PLA is mentioned as a biocompatible polymer in the literature; however, GO shows a cytotoxic effect depending on the dose. According to the direct cytotoxicity results, the non-toxicity of S1 and S2 samples can be explained by the biocompatibility of PLA and the correct selection of the concentration value for GO. Besides, the weak toxicity of PLA-G1, PLA-G2, and PLA-G3 samples can be explained by the high concentrations of clarithromycin and Se used in production. Effect of samples on L929 cell viability is examined by indirect method; It was observed that the samples did not show a toxic effect on the cells at any volume value, but a decrease in cell viability occurred due to the increasing volume ratio for all samples. PLA-G1, PLA-G2, and PLA-G3, which showed a slightly toxic effect in the direct cytotoxicity test, did not show cytotoxic effects because of indirect analysis. This can be explained by the diluted concentrations of Se and clarithromycin substances. It was observed that 25% volume of PLA-G3 showed the best viability (above the control) compared to other materials.

6.1.2. Cell adhesion and in vitro wound healing assay (scratch assay)

When the cell adhesion to the samples is examined (Figure 10), and it is shown that all 5 samples support the cell adhesion. The effect of samples; PLA, PLA-G, PLA-G1, PLA-G2, and PLA-G3 on L929 cell migration was compared with the control depending on the time. This situation may be related to the biocompatibility of PLA and the correct selection of the GO concentration value. In addition, cells treated with PLA-G1, PLA-G2, and PLA-G3 showed adhesion on the material, but stress granules and some dead cells were found in cells. This situation supports direct cytotoxicity results and can be explained by the excessive Se and clarithromycin concentrations added while the materials are being produced. When these effects are examined that the wounds formed in the control group and the groups exposed to the samples were closed after 24 h. In addition, it was observed that cells exposed to samples had a faster cell migration compared to the control group (Figure 11). Besides, it was observed that cells treated with PLA-GO nanofiber formulations that combined with Se (PLA-G1, PLA-G2, and PLA-G3) showed a faster migration. This situation can be explained by the antioxidant and anti-inflammatory effects of selenium.

The antibacterial activity against *E. coli*, *S. aureus*, *B. cereus,* and *S. epidermidis* were studied in PLA-G3 composites as shown in Figure 4. The bacteria were incubated in a growth medium with the pure PLA and the composites. The inhibition rates of the PLA-G2 and PLA-G3 had higher than other studies on *E. coli*, *S. aureus* and *B. cereus* (Figure 4a–c). Also, GO and Se combinations showed antibacterial effects on *S. epidermidis* and PLA-G2, PLA-G3 had excellent antibacterial effects on *S. epidermidis.* When the inhibition zone was 23.73 mm in the control group, 19.73 mm in Treatment 1, 19.87 mm in Treatment 2, 29.70 mm in PLA-G2, and 29,16 mm in PLA-G3 (Figure 4d). These results indicated that the antibacterial effect of the PLA and clarithromycin combinations have stronger than other combinations. Because clarithromycin is a macrolide antibiotic that binds to the 50S ribosomal subunit resulting in inhibition of protein synthesis of bacteria[50,51]. Therefore, combinations of the PLA and clarithromycin inhibited bacteria and showed a high antibacterial effect.

7. Conclusion

In this study, it was aimed to design effective wound dressing materials with antibacterial effects for diabetic wounds that are very difficult to heal by supporting the effects of GO and PLA with Se and clarithromycin. According to the results, nanofiber formulations have a high drug loading capacity, mechanical resistance, chemical stability, and large surface area.

This situation can be explained by the antioxidant and anti-inflammatory effects of Se. As a result, Se-supported wound dressing material supports the wound healing process and its use with clarithromycin provides an antibacterial effect on the environment. Using Se-supported PLA nanofibers as a wound dressing material will contribute to the wound healing process.

Acknowledgments

The work has been supported by the Yildiz Technical University Scientific Research Projects Coordination Department. The project number is FDK-2019-3531.

Funding

This work was funded by TUBITAK (The Scientific and Technological Research Council of Turkey) through the 2209-A Program under contract [number 1919B011800860].

References

[1] Moura, L. I. F.; Dias, A. M. A.; Carvalho, E.; De Sousa, H. C. Recent Advances on the Development of Wound Dressings for Diabetic Foot Ulcer Treatment – A Review. *Acta Biomater.* **2013**, *9*, 7093–7114. DOI: 10.1016/j.actbio.2013.03.033.

[2] Papanas, N.; Maltezos, E. Growth Factors in the Treatment of Diabetic Foot Ulcers: New Technologies, Any Promises? *Int. J. Lower Extrem. Wounds* **2007**, *6*, 37–53. DOI: 10.1177/1534734606298416.

[3] Subbiah, T.; Bhat, G. S.; Tock, R. W.; Parameswaran, S.; Ramkumar, S. S. Electrospinning of Nanofibers. *J. Appl. Polym. Sci.* **2005**, *96*, 557–569. DOI: 10.1002/app.21481.

[4] Sankaran, S.; Deshmukh, K.; Basheer Ahamed, M.; Khadheer Pasha, S. K. Electrospun Polymeric Nanofibers: Fundamental Aspects of Electrospinning Processes, Optimization of Electrospinning Parameters, Properties, and Applications. In *Lecture Notes in Bioengineering*; Sadasivuni, K., Ponnamma, D., Rajan, M., Ahmed, B., Al-Maadeed, M., Eds.; Springer: Cham, 2019. DOI: 10.1007/978-3-030-04741-2_12.

[5] Xue, J.; Wu, T.; Dai, Y.; Xia, Y. Electrospinning and Electrospun Nanofibers: Methods, Materials, and Applications. *Chem. Rev.* **2019**, *119*, 5298–5415. DOI: 10.1021/acs.chemrev.8b00593.

[6] Agarwal, S.; Wendorff, J. H.; Greiner, A. Use of Electrospinning Technique for Biomedical Applications. *Polymer* **2008**, *49*, 5603–5621. DOI: 10.1016/j.polymer.2008.09.014.

[7] Bhardwaj, N.; Kundu, S. C. Electrospinning: A Fascinating Fiber Fabrication Technique. *Biotechnol. Adv.* **2010**, *28*, 325–347. DOI: 10.1016/j.biotechadv.2010.01.004.

[8] Arriagada, P.; Palza, H.; Palma, P.; Flores, M.; Caviedes, P. Poly(Lactic Acid) Composites Based on Graphene Oxide Particles with Antibacterial Behavior Enhanced by Electrical Stimulus and Biocompatibility. *J. Biomed. Mater. Res.* **2018**, *106*, 1051–1060. DOI: 10.1002/jbm.a.36307.

[9] Bayer, I. S. Thermomechanical Properties of Polylactic Acid-Graphene Composites: A State-of-the-Art Review for Biomedical Applications. *Materials* **2017**, *10*, 748. DOI: 10.3390/ma10070748.

[10] Kanmaz, D.; Aylin Karahan Toprakci, H.; Olmez, H.; Toprakci, O. Electrospun Polylactic Acid Based Nanofibers for Biomedical Applications. *Mater. Sci. Res. India* **2018**, *15*, 12260. DOI: 10.13005/msri/150304.

[11] Thauvin, C.; Schwarz, B.; Delie, F.; Allémann, E. Functionalized PLA Polymers to Control Loading and/or Release Properties of Drug-Loaded Nanoparticles. *Int. J. Pharm.* **2018**, *548*, 771–777. DOI: 10.1016/j.ijpharm.2017.11.001.

[12] Kenawy, E. R.; Bowlin, G. L.; Mansfield, K.; Layman, J.; Simpson, D. G.; Sanders, E. H.; Wnek, G. E. Release of Tetracycline Hydrochloride from Electrospun Poly(Ethylene-Co-Vinylacetate), Poly(Lactic Acid), and a Blend. *J. Control. Release* **2002**, *81*, 57–64. DOI: 10.1016/S0168-3659(02)00041-X.

[13] Scaffaro, R.; Lopresti, F.; Marino, A.; Nostro, A. Antimicrobial Additives for Poly(Lactic Acid) Materials and Their Applications: Current State and Perspectives. *Appl. Microbiol. Biotechnol.* **2018**, *102*, 7739–7756. DOI: 10.1007/s00253-018-9220-1.

[14] Cheng, C.; Li, S.; Thomas, A.; Kotov, N. A.; Haag, R. Functional Graphene Nanomaterials Based Architectures: Biointeractions, Fabrications, and Emerging Biological Applications. *Chem. Rev.* **2017**, *117*, 1826–1914. DOI: 10.1021/acs.chemrev.6b00520.

[15] De Maio, F.; Palmieri, V.; Salustri, A.; Perini, G.; Sanguinetti, M.; De Spirito, M.; Delogu, G.; Papi, M. Graphene Oxide Prevents Mycobacteria Entry into Macrophages through Extracellular Entrapment. *Nanoscale Adv.* **2019**, *1*, 1421–1431. DOI: 10.1039/C8NA00413G.

[16] Ruiz, S.; Tamayo, J. A.; Ospina, J. D.; Porras, D. P. N.; Zapata, M. E. V.; Hernandez, J. H. M.; Valencia, C. H.; Zuluaga, F.; Tovar, C. D. G. Antimicrobial Films Based on Nanocomposites of Chitosan/Poly(Vinyl Alcohol)/Graphene Oxide for Biomedical Applications. *Biomolecules* **2019**, *9*, 109. DOI: 10.3390/biom9030109.

[17] Tran, P. A.; Webster, T. J. Antimicrobial Selenium Nanoparticle Coatings on Polymeric Medical Devices. *Nanotechnology* **2013**, *24*, 155101. DOI: 10.1088/0957-4484/24/15/155101.

[18] Wang, A.; Tang, Z.; Park, I. H.; Zhu, Y.; Patel, S.; Daley, G. Q.; Li, S. Induced Pluripotent Stem Cells for Neural Tissue Engineering. *Biomaterials* **2011**, *32*, 5023–5032. DOI: 10.1016/j.biomaterials.2011.03.070.

[19] Shakibaie, M.; Forootanfar, H.; Golkari, Y.; Mohammadi-Khorsand, T.; Shakibaie, M. R. Anti-Biofilm Activity of Biogenic Selenium Nanoparticles and Selenium Dioxide against Clinical Isolates of *Staphylococcus aureus*, *Pseudomonas aeruginosa*, and *Proteus mirabilis*. *J. Trace Elem. Med. Biol.* **2015**, *29*, 235–241. DOI: 10.1016/j.jtemb.2014.07.020.

[20] Sobczak, A. I. S.; Stefanowicz, F.; Pitt, S. J.; Ajjan, R. A.; Stewart, A. J. Total Plasma Magnesium, Zinc, Copper and Selenium Concentrations in Type-I and Type-II Diabetes. *Biometals*. **2019**, *32*, 123–138. DOI: 10.1007/s10534-018-00167-z.

[21] Andrews, P. J. D.; Avenell, A.; Noble, D. W.; Campbell, M. K.; Croal, B. L.; Simpson, W. G.; Vale, L. D.; Battison, C. G.; Jenkinson, D. J.; Cook, J. A. Randomised Trial of Glutamine, Selenium, or Both, to Supplement Parenteral Nutrition for Critically Ill Patients. *BMJ* **2011**, *342*, d1542–d1542. DOI: 10.1136/bmj.d1542.

[22] Santhosh Kumar, B.; Priyadarsini, K. I. Selenium Nutrition: How Important is It? *Biomed. Prev. Nutr.* **2014**, *4*, 333–341. DOI: 10.1016/j.bionut.2014.01.006.

[23] Clark, L. C.; Combs, G. F.; Turnbull, B. W.; Slate, E. H.; Chalker, D. K.; Chow, J.; Davis, L. S.; Glover, R. A.; Graham, G. F.; Gross, E. G.; et al. Effects of Selenium Supplementation for Cancer Prevention in Patients with Carcinoma of the Skin: A Randomized Controlled Trial. *J. Am. Med. Assoc.* **1996**, *276*, 1957. DOI: 10.1001/jama.276.24.1957.

[24] Kim, J.; Chung, H. S.; Choi, M. K.; Roh, Y. K.; Yoo, H. J.; Park, J. H.; Kim, D. S.; Yu, J. M.; Moon, S. Association between Serum Selenium Level and the Presence of Diabetes Mellitus: A Meta-Analysis of Observational Studies. *Diabetes Metab. J.* **2019**, *43*, 447–460. DOI: 10.4093/dmj.2018.0123.

[25] Jacobs, E.; Lance, P.; Mandarino, L.; Ellis, N.; Chow, H.-H.; Foote, J.; Martinez, J.; Hsu, C.-H.; Batai, K.; Saboda, K.; et al. Selenium Supplementation and Insulin Resistance in a Randomized, Clinical Trial. *BMJ Open Diabetes Res. Care* **2019**, *7*, e000613. DOI: 10.1136/bmjdrc-2018-000613.

[26] Anderson, R.; Joone, G.; Van Rensburg, C. E. J. An in-Vitro Evaluation of the Cellular Uptake and Infraphagocytic Bioactivity of Clarithromycin (A-56268, TE-031), a New Macrolide Antimicrobial Agent. *J. Antimicrob. Chemother.* **1988**, *6*, 923–933. DOI: 10.1093/jac/22.6.923.

[27] Gotfried, M. H. Clarithromycin (Biaxin®) Extended-Release Tablet: A Therapeutic Review. *Exp. Rev. Anti-Infect. Ther.* **2003**, *1*, 9–20. DOI: 10.1586/14787210.1.1.9.

[28] Darkes, M. J. M.; Perry, C. M. Clarithromycin Extended-Release Tablet: A Review of Its Use in the Management of Respiratory Track Infections. *Am. J. Respir. Med.* **2003**, *2*, 175–201. DOI: 10.1007/BF03256648.

[29] Chodosh, S.; Schreurs, A.; Siami, G.; Barkman, H. W.; Anzueto, A.; Shan, M.; Moesker, H.; Stack, T.; Kowalsky, S. Efficacy of Oral Ciprofloxacin vs. Clarithromycin for Treatment of Acute Bacterial Exacerbations of Chronic Bronchitis. *Clin. Infect. Dis.* **1998**, *27*, 730–738. DOI: 10.1086/514934.

[30] Anderson, G. Clarithromycin in the Treatment of Community-Acquired Lower Respiratory Tract Infections. *J. Hosp. Infect.* **1991**, *19*, 21–27. DOI: 10.1016/0195-6701(91)90214-S.

[31] Barry, A. L.; Fernandes, P. B.; Jorgensen, J. H.; Thornsberry, C.; Hardy, D. J.; Jones, R. N. Variability of Clarithromycin and Erythromycin Susceptibility Tests with Haemophilus Influenzae in Four Different Broth Media and Correlation with the Standard Disk Diffusion Test. *J. Clin. Microbiol.* **1988**, *26*, 2415–2420. DOI: 10.1128/JCM.26.11.2415-2420.1988.

[32] Barry, A. L.; Jones, R. N.; Thornsberry, C. In Vitro Activities of Azithromycin (CP 62,993), Clarithromycin (A-56268; TE-031), Erythromycin, Roxithromycin, and Clindamycin. *Antimicrob. Agents Chemother.* **1988**, *32*, 752–754. DOI: 10.1128/aac.32.5.752.

[33] CLSI. *Performance Standards for Antimicrobial Disk Susceptibility Test: Approved Atandard*; CLSI: Annapolis, MD, 2012.

[34] Balouiri, M.; Sadiki, M.; Ibnsouda, S. K. Methods for in Vitro Evaluating Antimicrobial Activity: A Review. *J. Pharm. Anal.* **2016**, *6*, 71–79. DOI: 10.1016/j.jpha.2015.11.005.

[35] Taylor, G.; Dyke, M. D. Van, Electrically Driven Jets. *Proc. Roy. Soc. Lond. A* **1969**, *313*, 453–475.

[36] Ramakrishna, S.; Mayer, J.; Wintermantel, E.; Leong, K. W. Biomedical Applications of Polymer-Composite Materials: A Review. *Compos. Sci. Technol.* **2001**, *61*, 1189–1224. DOI: 10.1016/S0266-3538(00)00241-4.

[37] Zeng, J.; Yang, L.; Liang, Q.; Zhang, X.; Guan, H.; Xu, X.; Chen, X.; Jing, X. Influence of the Drug Compatibility with Polymer Solution on the Release Kinetics of Electrospun Fiber Formulation. *J. Control. Release* **2005**, *105*, 43–51. DOI: 10.1016/j.jconrel.2005.02.024.

[38] Beachley, V.; Wen, X. Polymer Nanofibrous Structures: Fabrication, Biofunctionalization, and Cell Interactions. *Prog. Polym. Sci.* **2010**, *35*, 868–892. DOI: 10.1016/j.progpolymsci.2010.03.003.

[39] Wen, M. H.; Cheng, P. W.; Liao, L. J.; Chou, H. W.; Wang, C. Te, Treatment Outcomes of Injection Laryngoplasty Using Cross-Linked Porcine Collagen and Hyaluronic Acid. *Otolaryngol. Head Neck Surg.* **2013**, *149*, 900–906. DOI: 10.1177/0194599813508082.

[40] Kaialy, W.; Emami, P.; Asare-Addo, K.; Shojaee, S.; Nokhodchi, A. Psyllium: A Promising Polymer for Sustained Release Formulations in Combination with HPMC Polymers. *Pharm. Dev. Technol.* **2014**, *19*, 259–277. DOI: 10.3109/10837450.2013.775156.

[41] Qian, Y. F.; Su, Y.; Li, X. Q.; Wang, H. S.; He, C. L. Electrospinning of Polymethyl Methacrylate Nanofibres in Different Solvents. *Iran. Polym. J.* **2010**, *19*, 123–129.

[42] Huang, Y. S.; Lu, Y. J.; Chen, J. P. Magnetic Graphene Oxide as a Carrier for Targeted Delivery of Chemotherapy Drugs in Cancer Therapy. *J. Magn. Magn. Mater.* **2017**, *427*, 34–40. DOI: 10.1016/j.jmmm.2016.10.042.

[43] Buschle-Diller, G.; Cooper, J.; Xie, Z.; Wu, Y.; Waldrup, J.; Ren, X. Release of Antibiotics from Electrospun Bicomponent Fibers. *Cellulose* **2007**, *14*, 553–562. DOI: 10.1007/s10570-007-9183-3.

[44] Chung, S.; Ercan, B.; Webster, T. J.; Tran, P. Electrospun Silk Doped with Selenium for Antibacterial Skin Applications. Proceedings of the IEEE Annual Northeast Bioengineering Conference, NEBEC; 2014. DOI: 10.1109/NEBEC.2014.6972758.

[45] Mahmoudvand, H.; Fasihi Harandi, M.; Shakibaie, M.; Aflatoonian, M. R.; ZiaAli, N.; Makki, M. S.; Jahanbakhsh, S. Scolicidal Effects of Biogenic Selenium Nanoparticles against Protoscolices of Hydatid Cysts. *Int. J. Surg.* **2014**, *12*, 399–403. DOI: 10.1016/j.ijsu.2014.03.017.

[46] Balusamy, B.; Senthamizhan, A.; Uyar, T. Electrospun Nanofibrous Materials for Wound Healing Applications. In *Electrospun Materials for Tissue Engineering and Biomedical Applications: Research, Design and Commercialization*; Uyar, T.; Kny, E., Eds.; Woodhead Publishing: Amsterdam, 2017; pp 147–177. DOI: 10.1016/B978-0-08-101022-8.00012-0.

[47] Lim, C. T.; Tan, E.; Ng, S. Effects of Crystalline Morphology on the Tensile Properties of Electrospun Polymer Nanofibers. *Appl. Phys. Lett.* **2008**, *92*, 141908. DOI: 10.1063/1.2857478.

[48] Zhang, C.; Wang, L.; Zhai, T.; Wang, X.; Dan, Y.; Turng, L. S. The Surface Grafting of Graphene Oxide with Poly(Ethylene Glycol) as a Reinforcement for Poly(Lactic Acid) Nanocomposite Scaffolds for Potential Tissue Engineering Applications. *J. Mech. Behav. Biomed. Mater.* **2016**, *53*, 403–413. DOI: 10.1016/j.jmbbm.2015.08.043.

[49] Davoodi, A. H.; Mazinani, S.; Sharif, F.; Ranaei-Siadat, S. O. GO Nanosheets Localization by Morphological Study on PLA-GO Electrospun Nanocomposite Nanofibers. *J. Polym. Res.* **2018**, *25*, 24. DOI: 10.1007/s10965-018-1589-0.

[50] Piscitelli, S. C.; Danziger, L. H.; Rodvold, K. A. Clarithromycin and Azithromycin: New Macrolide Antibiotics. *Clin. Pharm.* **1992**, *11*, 137–152.

[51] Amsden, G. W. Erythromycin, Clarithromycin, and Azithromycin: Are the Differences Real? *Clin. Ther.* **1996**, *18*, P56–P72. DOI: 10.1016/S0149-2918(96)80179-2.